



## Enhanced photocatalytic and microbial activity of bio synthesized CdO tetrahedral clogs using Hibiscus rosa sinensis leaf extract

Gopi Somasundaram <sup>°</sup>, Jayaprakash Rajan <sup>\*†</sup>

<sup>°</sup> Nanotechnology Laboratory, Department of Physics, Sri Ramakrishna Mission Vidyalaya College of Arts and Science, Coimbatore-641020, India.

<sup>\*</sup> Corresponding Email: [jayaprakash.rajan.2015@gmail.com](mailto:jayaprakash.rajan.2015@gmail.com)

Received: 17-03-2022, Revised: 02-05-2022, Accepted: 05-05-2022, Published: 12-05-2022

**Abstract:** Green extracts from plants, fruits, flowers are being explored worldwide to minimize the effect of toxic chemicals used in nanoparticles fabrication. The present work is based on the cadmium oxide nanoparticles (CdO NPs) were synthesized using Hibiscus rosa sinensis leaf extract at different volume concentration of 10 ml, 20 ml, 30 ml, 40 ml and 50 ml under bio synthesis process. The prepared samples were characterized by XRD, UV-DRS, PL, FT-IR, FE-SEM, EDX, HR-TEM analysis. The XRD pattern confirms the cubic structure with average particle size of 41.48 nm to 51.69 nm. The estimated band gap energy is found in the range 2.19 eV to 1.67 eV. Near UV and violet emission in PL spectrum leads the presence of crystal defects in CdO lattice. Presence of vibrational modes of chemical species in the samples, are characterized by Fourier Transform Infrared (FT-IR) spectrum. The elemental compositions are detected by using energy dispersive X-Ray analysis (EDAX). The particle size and morphology with intense magnification is confirmed by FE-SEM and TEM- SAED analysis. The antibacterial and fungal activities of Hibiscus rosa sinensis leaf extract CdO nanoparticles are tested for different bacterial organisms like Staphylococcus aureus, Bacillus subtilis, Escherichia coli and Salmonella paratyphi and fungal organism like Candida albicans, Aspergillus niger and Aspergillus fumigates under the zone inhabitation method. The photocatalytic activities of the CdO samples on degradation of Methylene Blue azo dye under UV light irradiation are also studied.




**Keywords:** Hibiscus rosa sinensis, Green method, Tetrahedral clogs, Microbial.

### Introduction

The synthesis of nanoparticles under the eco-friendly method is an added advantage in the development of nanotechnology. Nowadays, the growing trend of nanomaterials must need an attention towards environment aspect. The synthesis process can at least reduce the pollution and support to produce the novelty in application in various fields. There are plenty of

conventional methods adopted to produce CdO nanoparticles such as microwave-assisted combustion method [1], co-precipitation [2], sonochemical method [3], sol-gel [4] and chemical precipitation [5]. The environmental friendly green synthesis technology is supported well for preparing metal oxide nanoparticles. The natural extracts from plants are used for preparation of metal oxide nanoparticles [6]. Unfortunately, many attempts have not been made on CdO nanoparticles due to its toxic nature. Recently a few research works has been carried out to investigate the various natural extracts to preparing cadmium oxide nanoparticles and it is shown in **Table 1**. The high electrical conductivity and higher optical transmittance of CdO nanoparticles make it is a suitable for future photocatalyst. While adopting the natural extract CdO nanoparticles it becomes less toxic nature and good photocatalyst (complete removal of organic dyes). There are many review works which are also reported on green and bio synthesis of ZnO nanoparticles by using natural material extraction from plants and microbes [30]. Some more recent articles of ZnO nanoparticles like *Pongamia pinnata* leaf [7], *Hibiscus rosa sinensis* [8], *Trifolium pretense* flower [9], *Tamarindus indica* leaf [10], *Plectranthus amboinicus* leaf extract [11], *Tribulus terrestris* leaf [12], *Rosa canina* fruit [13], *Sapindus rarak* rinds [14], *Solanum nigrum* leaf [15], *N-nitrosamines (TSNA)* tobacco extract [16], *Agathosma betulina* [17].

**Table 1** various natural extracts to preparing cadmium oxide nanoparticles

S.No	Nano particles	Particle size(nm)	Natural extract	Morphology	Figure	Application	Reference
1.	CdO	113 nm	<i>Hibiscus sabdariffa</i> flower extract	Cuboid shape		***	[17]
2.	CdO	5-17 nm	<i>Epigallocatechin gallate (EGCG)</i>	Raspberry shape		***	[16]
3.	CdO	25-50 nm	<i>Agathosma betulina</i> leaf	Quasi spherical shape		***	[15]

The usage of such type of plant extraction on CuO nanoparticles [18], Titanium oxide nanoparticles [19], silver nanoparticles [20] and gold nanoparticles [21] are more feasible as well as they were prepared under eco-friendly alternative method on reducing the toxicity during the preparation. The method of preparation on green synthesis is cost effective. The metal oxide nanoparticles prepared under this aspect possessed useful electrical and optical properties [22, 23]. The changes in morphology due to plant extraction are also reported in previous literature

[24]. Tokeer Ahamad et.al has investigated the antibacterial and antifungal activity on using metal oxide nanoparticles [25].

The green synthesis process is delivered the metal oxide nanoparticles due to active ingredients from the plant extract. *Hibiscus rosa sinensis* is an herbal plant which is coming under the malvaceae family. The biochemical constituents of the plants are taraxerolacetate,  $\beta$ -sitosterolcampesterol, stigmasterol, ergosterol, lipids, citric, tartaric acid, fructose, glucose, sucrose, flavonoids and flavonoid glycosides [26]. The *HRS* leaf extract has been used as the reducing as well as surface stabilizing agent for the synthesis of nanoparticles [27].

The present work is focused on the preparation of CdO nanoparticles using *HRS* leaf extract. The honey mediated combustion process with *HRS* surfactant is adopted in this approach which is not followed so far for the preparation of CdO nanoparticles. Most of the researchers adopted the direct heating method for preparation of CdO nanoparticles especially for metal oxide nanoparticles [28]. The morphological influence due to green extract is not discussed at an expected level by the earlier researchers so far [29]. The present preparation method is created the specific morphological change in the CdO nanoparticles formation. The semiconductor behavior of the green synthesized CdO nanoparticles is characterized by XRD, FT-IR, UV-DRS, SEM, EDX, HR-TEM and Photocatalytic activity.

## Methods of preparation

### Preparation of *HRS* leaf extract

*Hibiscus rosa sinensis* leaf were washed with tap water initially and then deionized water three times for the removal of unwanted dust. A 25g of leaves were cut into very small pieces. 40 ml of deionized water was added into it. This mixture was grained well. A green colored coagulated form of liquid was obtained and filtered it by using wire mesh filter that was cooled to a temperature of 23°C. The obtained coagulated *Hibiscus rosa sinensis* (*HRS*) extract was considered for the synthesis process of CdO nanoparticles.

## Materials and Synthesis of CdO Nanoparticles

Materials considered for synthesis of CdO nanoparticles were *Hibiscus rosa sinensis* (*HRS*) Leaf, cadmium nitrate  $[\text{Cd}(\text{NO}_3)_2] \cdot 6\text{H}_2\text{O}$ , honey ( $\text{C}_{12}\text{H}_{22}\text{O}_{11}$ ) and deionized water. The precursor solution, 0.2 M was prepared by dissolving of cadmium nitrate  $[\text{Cd}(\text{NO}_3)_2] \cdot 6\text{H}_2\text{O}$ . 150ml of deionized water and stirred for 3 hours at room temperature. An aqueous solution of honey was mixed with the cadmium nitrate solution. The mixed solution was placed on a hot plate with continuous stirring at 100°C. During evaporation, the solution formed a very viscous gel. The gel was then heated to 150°C to initiate a self-sustaining combustion reaction and to produce an as-prepared CdO powder. The main ingredient of honey, i.e., glucose and fructose, are "single" sugars or monosaccharides. These monosaccharides have the same molecular formula ( $\text{C}_6\text{H}_{12}\text{O}_6$ ), but the arrangements of the atoms are different [50, 51]. After the CdO with honey gel precursor was heated at a temperature of 350°C, the decomposition of glucose and

fructose occurred with the release of nitrogen and carbon dioxide gases. Finally, 10ml, 20 ml, 30 ml, 40 ml and 50 ml of *HRS* leaf extract was titrated at the main solution. Under continuous stirring, a change in the color of the reaction mixture was observed from normal transparent colour into light green. The stirring was further continued for another 1hour. Then the mixture was heated at 100 °C using magnetic stirrer. A burned powder was obtained at the bottom of the flask. The powder is further annealed at 400° C. The black brown colour powder was obtained as final yield.

### Characterization technique of CdO nanoparticles

The *HRS* leaf extract CdO nanoparticles was characterized with an X-ray powder diffractometer, Rigaku X-ray diffraction unit model ULTIMA (III).The morphology and atomic percentage of CdO nanoparticles was measured by using Scanning Electron Microscope (SEM) and Energy Dispersive X-ray analysis (EDAX) by using JOEL 5600LV microscope at an accelerating voltage of 10 kV. The morphology and size of the products were observed by High resolution transmission electron microscopy (HRTEM) and selected-area electron diffraction (SAED) was recorded for the sample on a Technai G20-stwin using an accelerating voltage of 200 kV. The Fourier transform infrared (FT-IR) spectra using KBr and the spectrum was recorded by using a JASCO (FP8300, Japan) spectrometer. Ultraviolet (UV-vis) absorption spectrum was also recorded by using JASCO (V-770, Japan) Spectrophotometer. Photoluminescence (PL) measurements were carried out at room temperature using JASCO Spectrofluorometer (Model FP8300, Japan) equipped with a Xenon lamp.

### Antibacterial and antifungal study

Gopi somasundaram et.al [54] reported the previous article that antibacterial and antifungal activity of biosynthesized CdO nanoparticles was tested against bacterial pathogens like gram positive (*Staphylococcus aureus*, *Bacillus subtilis*) and gram negative (*Escherichia coli*, *Salmonella paratyphi*) by zone inhibition method. Agar plates of test organisms were prepared by dipping a sterile in the inoculums. The swab is placed over the agar surface. The inoculums are dried at room temperature by closing it with lid. Later, the discs were placed on the agar plates and *HRS* leaf extract CdO nanoparticles. Pure *HRS* leaf extract, reference sample of Ciprofloxacin(100µg) were loaded onto each disc in each petri plate of respective pathogens, followed by incubation for 24 hours and zone of inhibition was measured with a meter ruler around each disc in mm. The similar procedure was adopted for analyzing the zone inhibition of antifungal activity. In this process the sample of biosynthesized CdO nanoparticles, Pure *HRS* leaf extract and reference sample of clotrimazole (100µg) were determined by the same zone inhibition method described earlier against three fungal test cultures like *Candida albicans*, *Aspergillus niger*, *Aspergillus fumigatus*.

## Photocatalytic assay

The photocatalytic activity of pure and various concentration of *HRS* leaf extract CdO nanoparticles were investigated by the degradation of anionic and cationic nature of the methylene blue in aqueous medium under UV visible light irradiation ( $\lambda = 236$  nm). In a typical photocatalytic experiment, 75 mg of pure and various concentration of *HRS* leaf extract CdO nanoparticles were added to the 100 ml aqueous methyl blue solution ( $10^{-4}$ ) and suspension was magnetically stirred for 20 minutes at room temperature. The irradiation was done using an 8W medium pressure mercury vapour lamp (Heber multi lamp photo reactor HML MP 88). The concentration of MB dye prior to irradiation was used as the initial value for the measurement of MB dye degradation. After a defined time interval of irradiation (30 min), 5 ml of solution was taken and tested by UV- vis absorption spectrum. At the end of the decolorization, the efficiency percentage was calculated from the formula,

$$\text{Decolorization efficiency (\%)} = \frac{X_0 - X}{X_0} \times 100$$

Where,  $X_0$  is the initial concentration of MB dye and  $X$  is the concentration of MB dye after irradiation.

## Results and discussion

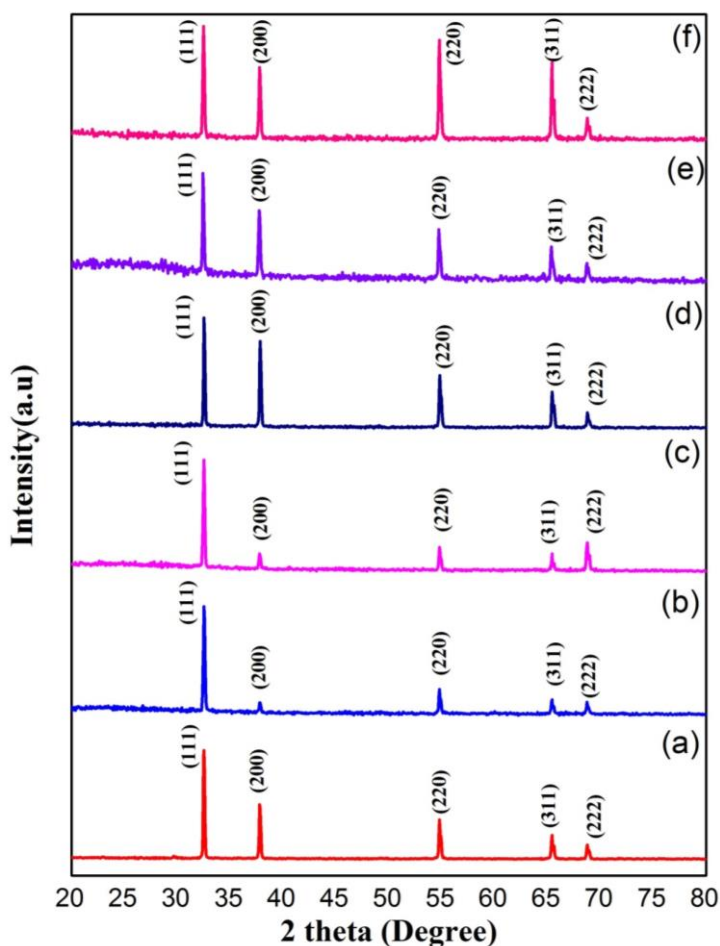
### XRD Analysis

Figure 1(a-f) shows that XRD pattern of without *HRS* leaf extract based CdO nanoparticles and with *HRS* extract of various volume such as 10, 20, 30, 40 and 50 ml calcinated at 400 °C. The XRD spectra of the sample indicates the number of strong diffraction peaks at the angles such as 33.1°, 38.4°, 55.4°, 66.0° and 69.3°, the corresponding reflection peaks belong to the (hkl) value such as (110), (200), (220), (311), and (222) [JCPDS 05- 0640]. These indexed peaks are confirmed the simple cubic structure. The main peak at 33.1° indicates the (110) crystallographic plane of *Hibiscus rosa sinensis* leaf extract CdO nanoparticles, which predominantly specifies the good crystalline nature of CdO nanoparticles. There is no additional diffraction peaks appeared for other species in the samples and it confirmed the prepared cadmium oxide nanoparticles with the help of *HRS* leaf extract free from impurities. It means that additions of biological product during the preparation are supporting well to achieve good crystallinity under relevant process of heating. Similarly, the influence of change in concentration of *HRS* leaf extract was also analyzed from the XRD pattern and it is shown in the Fig (b, c, d, e and f). The reflection peaks as appeared for the sample (b) such as (110), (200), (220), (311), and (222) are indicated that good crystalline nature [30,54]. The peak (110), (200), (220), (311), and (222) belongs to similarly at sample (c, d and f) are also posses similar hkl value and indicates the good crystalline nature of the sample. The change in crystalline size is observed for the sample b, c, d and f. This change is due to the green *HRS* extract of various volume of concentration. These green extract helps to increase the grain size. The biological additive of *HRS* extract is controlled the nucleation with growth of particle. The sharp diffraction peaks at 33.1° and 38.4°

indicated that the crystalline size of CdO nanoparticles was very small and in nano range. The remaining diffraction peaks ( $55.4^\circ$ ,  $66.0^\circ$  and  $69.3^\circ$ ) indicates the high crystalline and increase the grain size. The average particle size of the biosynthesized CdO nanoparticles was determined using Debye- Scherrer's formula [31];

$$D = \frac{K\lambda}{\beta \cos\theta} (\text{\AA})$$

Where D is the average crystallite size in  $\text{\AA}$ ,  $k=0.9$  is the shape factor,  $\lambda$  is the wave length of X-ray Cu  $K\alpha$  radiation ( $1.5406\text{\AA}$ ),  $\theta$  is the Bragg diffraction angle,  $\beta$  is the full width at half maximum (FWHM), of the respective diffraction peak. The crystalline sizes are predicted as 40.1nm for pure, 41.68 nm for 10ml extract, 48.49 nm for 20ml extract, 49.85 nm for 30ml extract, 50.48 nm for 40ml extract and 51.69 nm for 50ml extract.



**Figure 1** XRD pattern of (a) Pure and (b-f) *HRS* leaf extract CdO nanoparticles

## Optical properties

### UV-vis DRS

The UV absorption spectra of pure CdO nanoparticles and *HRS* biosynthesized CdO nanoparticles with various volume concentrations of 10ml -50ml is shown in fig. 2(a-f). In this, spectra noted that the absorption of pure CdO is in the UV region with a band edge at 253nm. However 10ml, 20ml, 30ml, 40ml and 50 ml of *HRS* CdO nanoparticles, the optical absorption of these nanoparticles extends into visible region and range is from 200-400nm. As compared to the spectrum of pure and various volume of CdO nanoparticles exhibit the same intensity and slight variation of wavelength but strong absorption in the visible region. The minimum absorption at 240 nm which can be assigned to the intrinsic bandgap absorption of CdO nanoparticles due to the electron transitions from valence band to conduction band ( $O_{2p}$ -  $Cd_{3d}$ ) [32]. The UV vis diffuse reflectance spectra of the bio synthesized CdO nanoparticles are shown in Fig 3(a-f). The reflectance (R) was converted into absorption by Kubelka-Munk function  $F(R)$  [33]. The optical bandgap ( $E_g$ ) was obtained by the modified K-M function  $[F(R)hv]^2$  versus the photon energy.

$$[F(R) hv]^2 = [(1-R)^2/2R * hv]^2$$

The bandgap energies of pure and various volume of *HRS* leaf extract CdO nanoparticles were calculated. The bandgap diagrams and values are shown in Fig. 3 b(a-f). The results reveal that optical bandgap value varied with the pure and various volume of *HRS* leaf extract CdO nanoparticles exhibit the bandgap energy was 2.19 eV, 1.95 eV, 1.82 eV, 1.79 eV, 1.71eV and 1.67eV for pure, 10ml, 20ml, 30ml, 40ml and 50ml respectively. This has good agreement with the bandgap energy value of standard CdO nanoparticles [34].

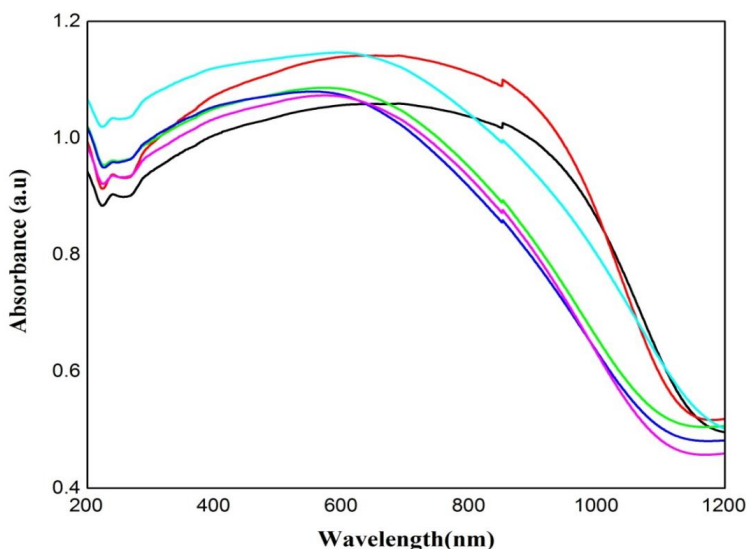


**Figure 2.** UV absorption Spectrum of Pure and *HRS* leaf extract CdO nanoparticles

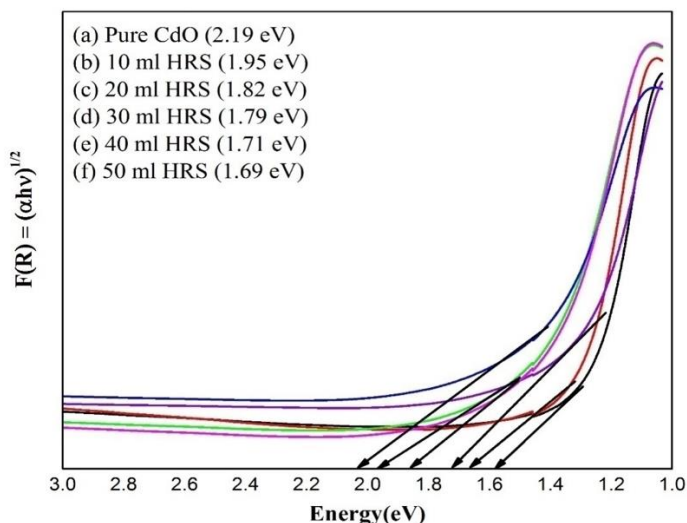


**Figure 3.** UV-DRS Spectra of (a) Pure and (b-f) *HRS* leaf extract CdO nanoparticles

Optical bandgap value was decreased with increasing the volume of *HRS* leaf extract concentration, which is commonly from the valence band to conduction band of nanostructure, or particles that have wide particle size distribution [35]. This also reveals that there is the change in the bandgap and surface modification of CdO as pure into various concentrations. However, a small difference in band gap energy ( $E_g$ ) value was noticed due to various parameters such as the biosynthesis of *Hibiscus rosa sinensis* colloidal extract, crystallinity, particle size, morphology, surface area etc.

### PL analysis

The fluorescence spectra of CdO nanoparticles synthesized at pure and various concentration of *Hibiscus rosa sinensis* leaf extract are shown in Fig 4(a-f). The pure CdO nanoparticles of luminescence spectra 4(a) exhibit strong emission peak at 417 nm and 10 ml, 20 ml, 30 ml, 40 ml and 50 ml of *HRS* leaf extract CdO nanoparticles shown in Fig 4(b-d) exhibit the same emission shift at 417 nm with excitation of 330 nm and slight variation of intensity. The peak at 417 nm corresponds to the violet region of CdO nanoparticles. This emission is assigned to the transition between photo-generated holes and singly ionized oxygen vacancies. Surface states are also a factor, which may seriously influence the PL properties in nanomaterials due to their large surface to volume ratio. In addition, surface dislocations are another factor, which might play a role in the intense visible emission for the nanoparticles. The peak at 529 nm and 609 nm belongs to the strong green and orange shift which is due to the effect of change in surface state or particle size and formation of the acceptor and donor states in the region between the valence and conduction band [36]. This figure shows the decrease in the emission intensity with adding the *HRS leaf* extract concentration (10- 50 ml) in the reaction medium.



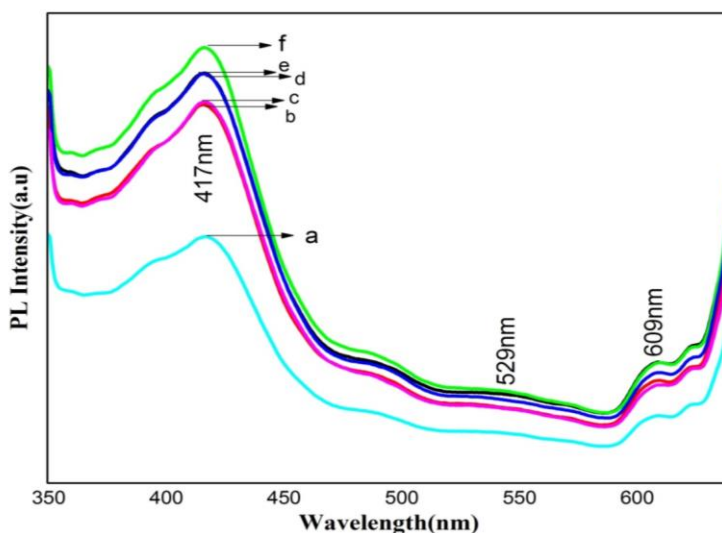


**Figure 4.** PL Emission Spectrums of (a) Pure and (b-f) HRS leaf extract CdO nanoparticles

### FT-IR Analysis

The FT-IR spectrum of pure and various concentration of *HRS* leaf extract CdO nanoparticles shown in Fig 5 (a-f). The spectrum of sample 5(f) indicates the vibration bands at  $3780.10\text{ cm}^{-1}$ ,  $2362.37\text{ cm}^{-1}$ ,  $1586.16\text{ cm}^{-1}$ ,  $1384.60\text{ cm}^{-1}$  and  $483.08\text{ cm}^{-1}$  of Pure CdO nanoparticles shifts to  $3782.41\text{ cm}^{-1}$ ,  $2348.87\text{ cm}^{-1}$ ,  $1589.06\text{ cm}^{-1}$ ,  $1383.68\text{ cm}^{-1}$  and  $442.58\text{ cm}^{-1}$  for formation of CdO nanoparticles with various concentration (10-50 ml) of *HRS* leaf extract. In all the spectra Fig 5 (a-f) the broad vibrational band observed at  $3782.41\text{ cm}^{-1}$ ,  $3852.11\text{ cm}^{-1}$ ,  $3852.87\text{ cm}^{-1}$ ,  $3804.05\text{ cm}^{-1}$ ,  $3801.05\text{ cm}^{-1}$  and  $3780.10\text{ cm}^{-1}$  are indicating the presence of symmetric stretching modes of water molecules in hydrogen bonded O-H stretching vibration [37]. The sharp intense band presence of all spectra at  $2348.87\text{ cm}^{-1}$ ,  $2341.41\text{ cm}^{-1}$ ,  $2361.41\text{ cm}^{-1}$ ,  $2348.87\text{ cm}^{-1}$ ,  $2348.87\text{ cm}^{-1}$  and  $2362.37\text{ cm}^{-1}$  are observed in which indicates the O=C=O vibration of carbon dioxide [38]. The transmittance peaks at  $442.58\text{ cm}^{-1}$ ,  $433.90\text{ cm}^{-1}$ ,  $435.05\text{ cm}^{-1}$ ,  $483.08\text{ cm}^{-1}$ ,  $481.91\text{ cm}^{-1}$  and  $443.54\text{ cm}^{-1}$  corresponding to Cadmium- oxygen stretching mode of vibration [39]. The increase in particle size of CdO nanoparticles due to the effect of *HRS* leaf extract and without *HRS* extract is confirmed from this shift. This result is well agreed with the particle size variation observed from XRD analysis.

IR measurements were carried out to identify the possible biomolecules present in *HRS* leaf extract responsible for reduction and stabilization of the biosynthesized CdO nanoparticles. The vibrational band observed at  $3330\text{ cm}^{-1}$ ,  $2919\text{ cm}^{-1}$ ,  $1634\text{ cm}^{-1}$  and  $1080\text{ cm}^{-1}$  are show that alkaloids and flavonoids are the major biomolecules present in the *HRS* leaf extract [40] and this have adsorbed on the metal surface by the interaction with carbonyl group or keto group. In addition, the functional group in the *Hibiscus rosa sinensis* leaf extract have been oxidized during

the reaction of  $Cd(NO)_3$  to  $CdO$  nanoparticles [41]. The shifted transmittance peaks in the *HRS* leaf extract and  $CdO$  nanoparticles clearly indicates the nanoparticles formation by the leaf extract of *HRS* acts as stabilizing and reducing agent [42].

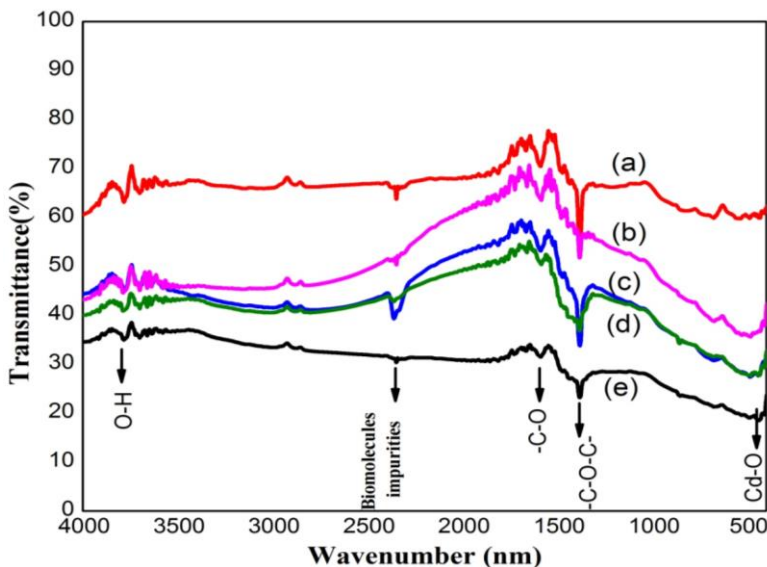


Figure 5. (a-e) FT-IR Spectrum of *HRS* leaf extract  $CdO$  nanoparticles

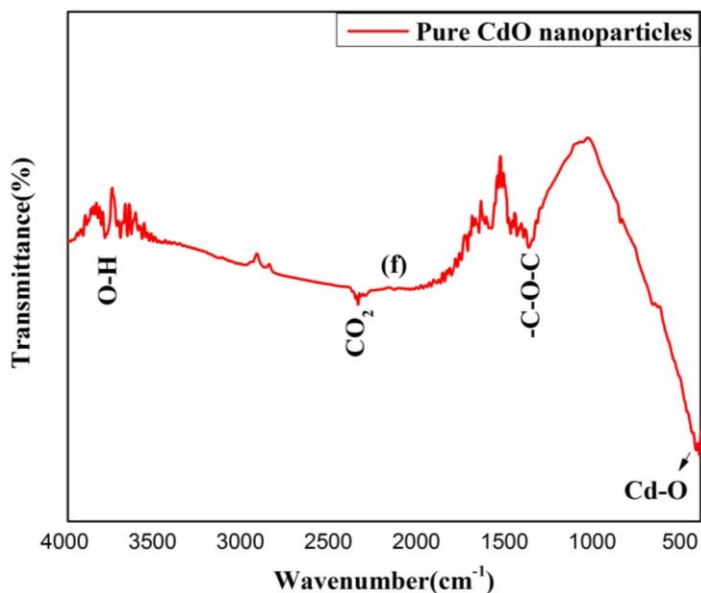


Figure 5. (f) FT-IR Spectrum of Pure  $CdO$  nanoparticles

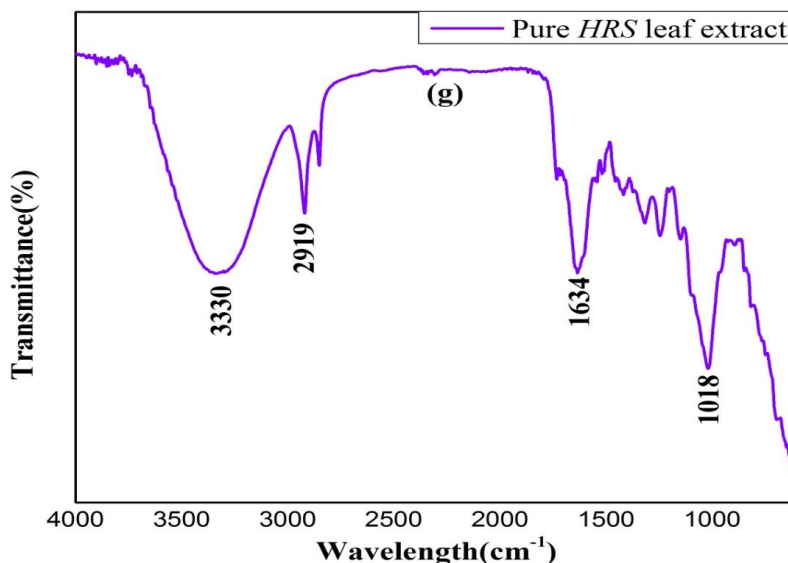


Figure 5 (g) FT-IR Spectrum of Pure *HRS* leaf extract

### SEM analysis

Fig 6(a-f) indicate the morphological analysis of pure and various concentration of *HRS* leaf extract CdO nanoparticles. These image shows that CdO nanoparticles have various morphological variation from pure to various extract concentration of 10, 20, 30, 40 and 50 ml respectively. Fig 6(a) shows the structure of the pure CdO nanoparticles exhibits the irregular and agglomerated as a result of polarity and electrostatic attraction of nanoparticles (there is no capping and stabilizing agent). When increasing the volume of *HRS* leaf extract is rising to 10 ml in which the morphology change of the CdO nanoparticles is begun and forms tetrahedral shaped clogs. It is evidently shows in Fig 6(b). Further, increasing the *HRS* leaf extract of 20 and 30 ml Fig 6(c-d) the same tetrahedral and octahedral morphologies are formed but less agglomerated patterns. On minute observation, Fig 6(e-f) shows the clear pyramid like structure end with sharp edges. The plane surface of the CdO tetrahedral clogs embedded with spherical particles and nano rods. This is clearly focused in HR-TEM images. The green synthesized CdO nanoparticles among the various concentration of *HRS* leaf extract, the 50 ml of the extract was found to influence more on morphological change and possessed fine crystallinity, uniform distribution, less agglomeration, clear tetrahedral shaped clogs. This formation reveals that the 50 ml of the *HRS* leaf extract was suitable as a reducing agent.

The possible formation process of CdO nanoparticles is predicted as following explanation. When cadmium nitrate mixed with hetro polysaccharides formed of proteins and polysaccharides. These are gel- like and are present in the extracellular matrix. Secondly, the extracellular react with metal oxide ions at a low temperature to form superstructure. The resulting networks undergo slow decomposition when subjected to heat treatment. In summary,

polysaccharides molecules that interact with divalent  $\text{Cd}^{2+}$  cations forming bridges between two hydroxyl groups from two various chain comes in close contact. The divalent ions keep the molecules to gather and form various structure of  $\text{CdO}$  [43]. This type of nanostructure is responsible for the conjugation of all these families of compounds present in the extract and exhibit a synergistic effect to get the various structures involves the steps of complex reaction nanoparticles aggregation formation, the burn of compounds present in the extract to form various morphologies.

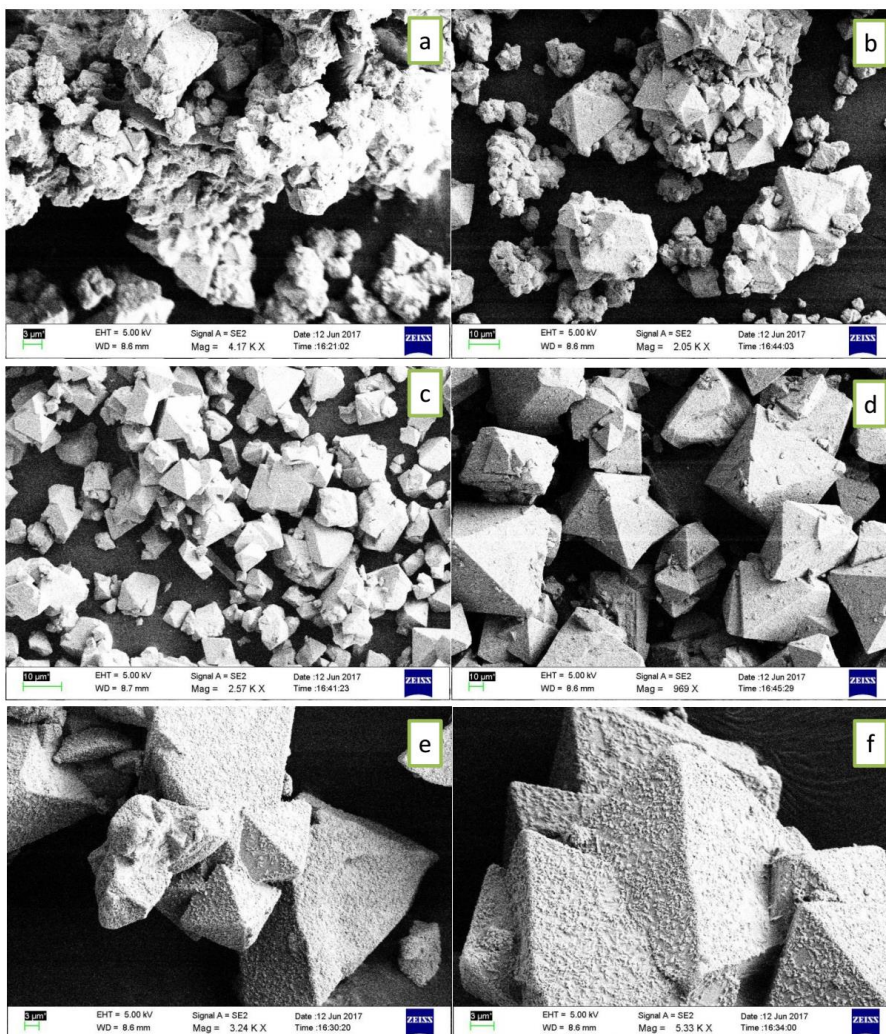


**Figure 6** shows the FE-SEM images of  $\text{CdO}$  nanoparticles (a) Pure and (b-f) 10-50 ml of *HRS* leaf extract

## EDX analysis

Fig 7(a-d) shows the EDX spectrum of Pure and various concentration of *HRS* leaf extract CdO nanoparticles. In the entire spectrum has strong peak at 0.3 KeV and 3.1 KeV corresponds to oxygen and cadmium present in the *HRS* leaf extract CdO nanoparticles. There are small impurity lines (Al, Na, Cu, C) are detected for the biosynthesized CdO nanoparticles. Because due to the temperature, precursor purity, natural extract or instrument coating.

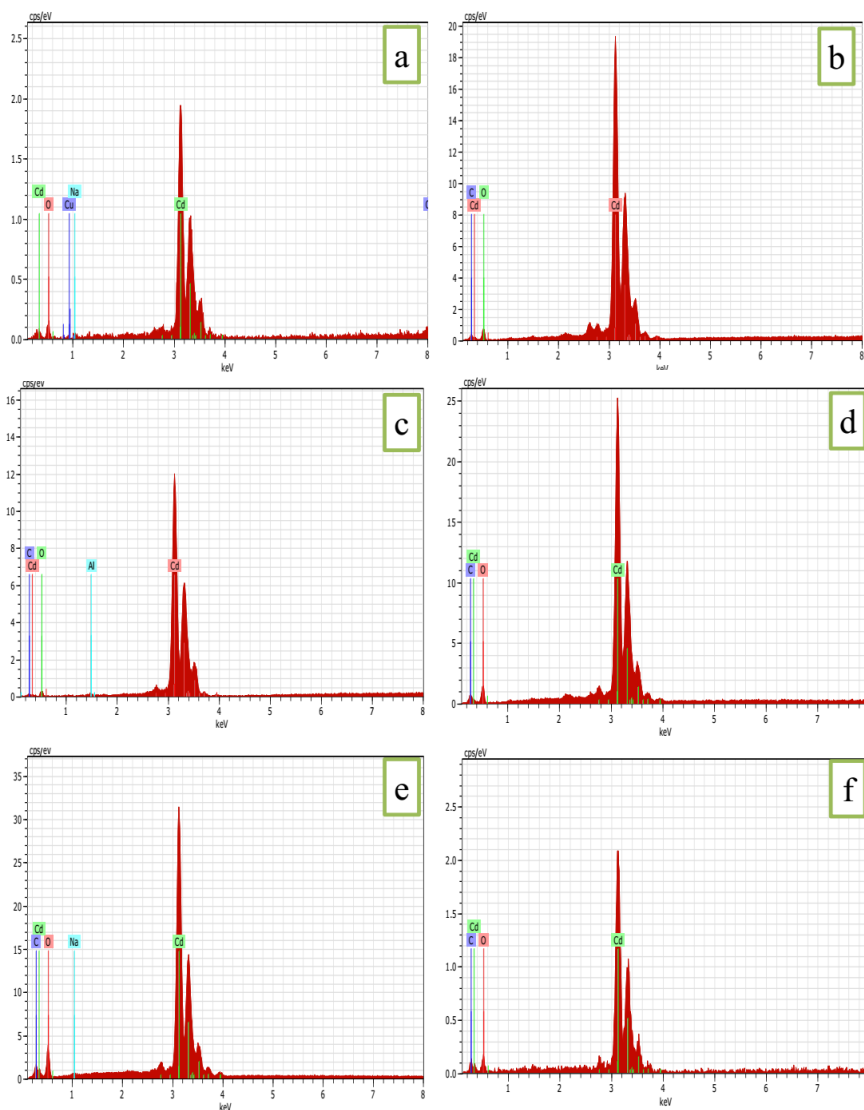


**Figure 7** shows the EDX spectrum of CdO nanoparticles (a) Pure and (b-f) 10-50 ml of *HRS* leaf extract

In all the spectrum, the emission of strong signals belongs to cadmium and oxygen as 60.87 % and 24.25 % for pure CdO nanoparticles and various concentration of *HRS* leaf extract CdO nanoparticles predicted as 51.62 % and 44.20 % for 10 ml, 50.60 % and 40.28 % for 20 ml, 54.12 % and 37.94 % for 30 ml, 64.64 % and 34.45 % for 40 ml, 56.43 % and 32.26 % for 50 ml. In overall observation of Cd and O atomic percentage is found to be decrease with increasing the *HRS* leaf extract concentration.

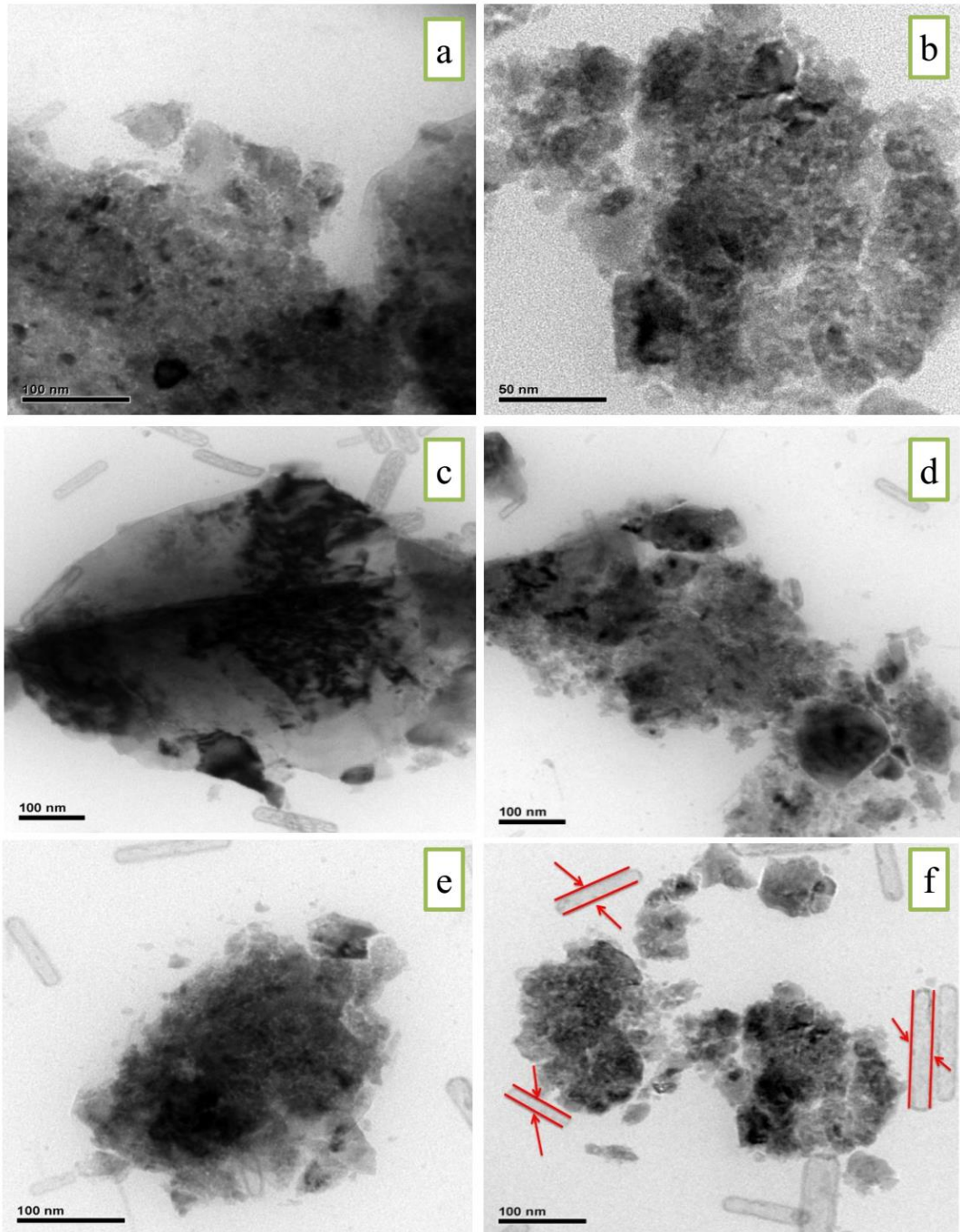
### HR-TEM analysis

Fig 8(a-f) shows the HR-TEM images of pure and various concentration of the *HRS* leaf extract CdO nanoparticles. All the images are summarizing the corresponding observation in terms of particle size, agglomeration status, structure and crystallinity. These images show that the dried powder consists of irregular, spherical and tube-shaped nanoparticles. There is no direct contact between the nanoparticles is evident in the HR-TEM images suggesting that some of the *HRS* molecules act as capping or stabilizing agents and prevents the agglomeration of the nanoparticles. Fig 8(a) shows the pure CdO nanoparticles exhibits the more agglomeration along with irregular shape. When increasing the *HRS* leaf extract, the particles are dispersed as well as individual identification of CdO nanoparticles are shown in Fig 8 (b-f). Fig 8(c) shows the precise magnification of TEM images are observed and the similarity of structured in the FE-SEM. The plane surface of the tetrahedral shape embedded with surface spherical particles. Fig 8(d-f) shows the more number of spherical particles stick on the plane surface of the tetrahedral shape and nano tubes within the size of  $\sim 55$  to 72 nm. The entire observation of the *HRS* leaf extract CdO nanoparticles showed that the particle size was in the range between 35 to 59 nm and nano tubes in the range of 48-85 nm.

Fig 8 (g) shows that significant degree of crystallinity. The d-spacing value is predicted from this image as 0.92 nm. The consistency of the crystalline nature of the CdO nanoparticles is well identified from SAED pattern of Fig 8(h). It also reveals that the good polycrystalline of the CdO nanoparticles with simple cubic structure. It is also identified from the XRD pattern of Fig. 1(a-f). The bright circular rings indicate corresponding plane such as (110), (200), (220), (311) and (222).

### Antibacterial and antifungal activities

The effect of *HRS* leaf extract mediated CdO nanoparticles as possible antibacterial agent, the plant extract and those mediated cadmium oxide nanoparticles were tested for respective antibacterial activities towards both gram positive (*Staphylococcus aureus*, *Bacillus subtilis*) and gram negative (*Escherichia coli*, *Salmonella paratyphi*) bacteria. The inhibition of CdO nanoparticles over the bacterial and fungal is discussed as follows. The gram positive bacteria cell wall is a peptidoglycan molecule. The gram positive bacteria cell consists of thick wall. As the Cd ions are positively charged and peptidoglycan is negative charged.



**Figure 8** shows the HR-TEM images of CdO nanoparticles (a) Pure and (b-f) 10-50 ml of *HRS* leaf extract

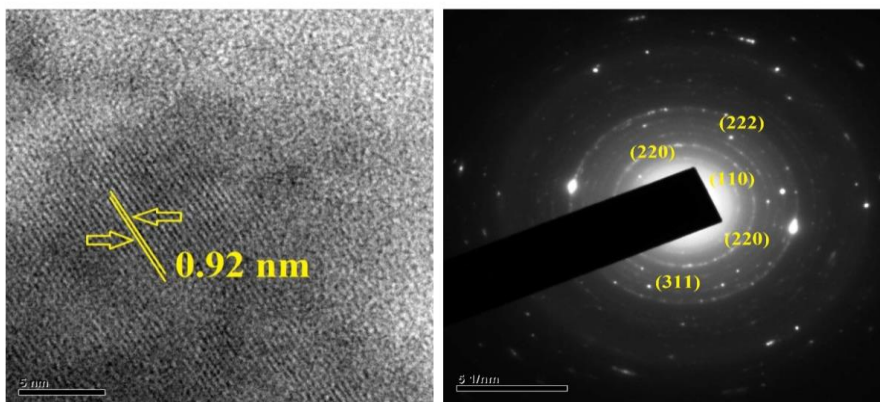


Figure 8 (g) shows the d- spacing and 8(h) SAED pattern of *HRS* leaf extract CdO nanoparticles

So there is a electrostatic attraction [44] between these positive and negative ions. There are more positive Cd ions are interacting over the surface of the peptidoglycan. The more accumulation of Cd ions over the surface damages the cell wall and diffuses into the cells. In this way the cell wall or membrane gets damaged. Fig (12) shows that the zone of inhibition for gram positive bacteria *Staphylococcus aureus* and *Bacillus subtilis* is observed as 8 mm and 9 mm. similarly the zone of inhibition of CdO nanoparticles on two gram negative bacteria of *Escherichia coli* and *Salmonella paratyphi* is observed as 8 mm and 9 mm. **Table 2** summarizes the antibacterial activity of *HRS* leaf extract CdO nanoparticles. Based on the zone of inhibition, biosynthesized CdO nanoparticles prove to the significant antibacterial activity against *Staphylococcus aureus*, *Bacillus subtilis*, *Escherichia coli* and *Salmonella paratyphi*. On the other side, control (standard) and leaf extract did not exhibit significant antibacterial activity. The result from the antibacterial activity is presumed from the inhibition as low activity over the bacterial medium. Thus, the zones around CdO nanoparticles are formed when the growth of the bacteria's are stopped by CdO nanoparticles cogently [45, 46].

Antifungal properties of biosynthesized CdO nanoparticles were also examined against selected fungal test pathogens such as *Candida albican*, *Aspergillus niger* and *Aspergillus fumigates* are shown in Fig. (12) The zone of inhibition of CdO nanoparticles with respect to all pathogens are listed in the **Table 3**. This test is proved that CdO nanoparticles possessed good antifungal activity towards *Candida albican* as 10 mm, *Aspergillus niger* as 08 mm and *Aspergillus fumigates* as 08 mm. The predominant zone inhibition due to CdO nanoparticles over the antifungal activity is observed. Also the absence of antifungal activity of the extract is identified. These results confirmed that the *HRS* leaf extract based CdO nanoparticles showed significant antibacterial capability against gram positive and gram negative bacteria as well as good antifungal activities.



**Table 2** Antibacterial activity of *HRS* leaf extract CdO nanoparticles

S.No.	Organisms bacteria	Zone of Inhibition(mm) Samples (100µg/disc)	
		Leaf Extract	CdO nanoparticles
1.	<i>Staphylococcus aureus</i>	-	08
2.	<i>Bacillus subtilis</i>	-	09
3.	<i>Escherichia coli</i>	-	08
4.	<i>Salmonella paratyphi</i>	-	09

**Table 3** The zone of inhibition of CdO nanoparticles with respect to all pathogens

S.No.	Organisms fungal	Zone of Inhibition(mm) Samples(100µg/disc)	
		Pure HRS extract	CdO nanoparticles
1.	<i>Candida albicans</i>	-	10
2.	<i>Aspergillus niger</i>	-	08
3.	<i>Aspergillus fumigatus</i>	-	08

### Photocatalytic activity

The photocatalytic activity of pure and various concentration of *HRS* leaf extract CdO nanoparticles were investigated for the aqueous solution of chromophoric structure of MB dye under UV light irradiation. The 50 ml of *HRS* leaf extract CdO nanoparticles exhibits the higher photocatalytic activity. The chromophoric absorption peak of MB dye at  $\sim 664$  nm is fixed to monitor the photodegradation of dye molecules. Fig 9 (a-f) shows the degradation of MB dye with pure CdO and various concentration of *HRS* leaf extract CdO nanoparticles under the wavelength  $\lambda=256$  nm.

From Fig 9 (a-f), it is clear that after exposing the mixed solution of MB dye and photocatalyst such as, CdO nanoparticles without natural extract and 10-50 ml of *HRS* leaf extract CdO nanoparticles under UV light irradiation for 120 min. The pure CdO nanoparticles degrade the MB dye up to 66.6 % similarly, the increase of MB dye for 10 ml of *HRS* CdO nanoparticles as 68.7 %, 20 ml of *HRS* CdO nanoparticles as 72 %, 30 ml of *HRS* CdO nanoparticles as 72.30 %, 40 ml of *HRS* CdO nanoparticles as 74.41 % and 50 ml of *HRS* CdO nanoparticles as 91.8 % are observed from the UV light irradiation. These results confirm that

the pure CdO nanoparticles has intrinsic photocatalytic activity is gradually enhanced by adding *HRS* leaf extract. The degradation of MB dye is not observed in the absence of photocatalyst.

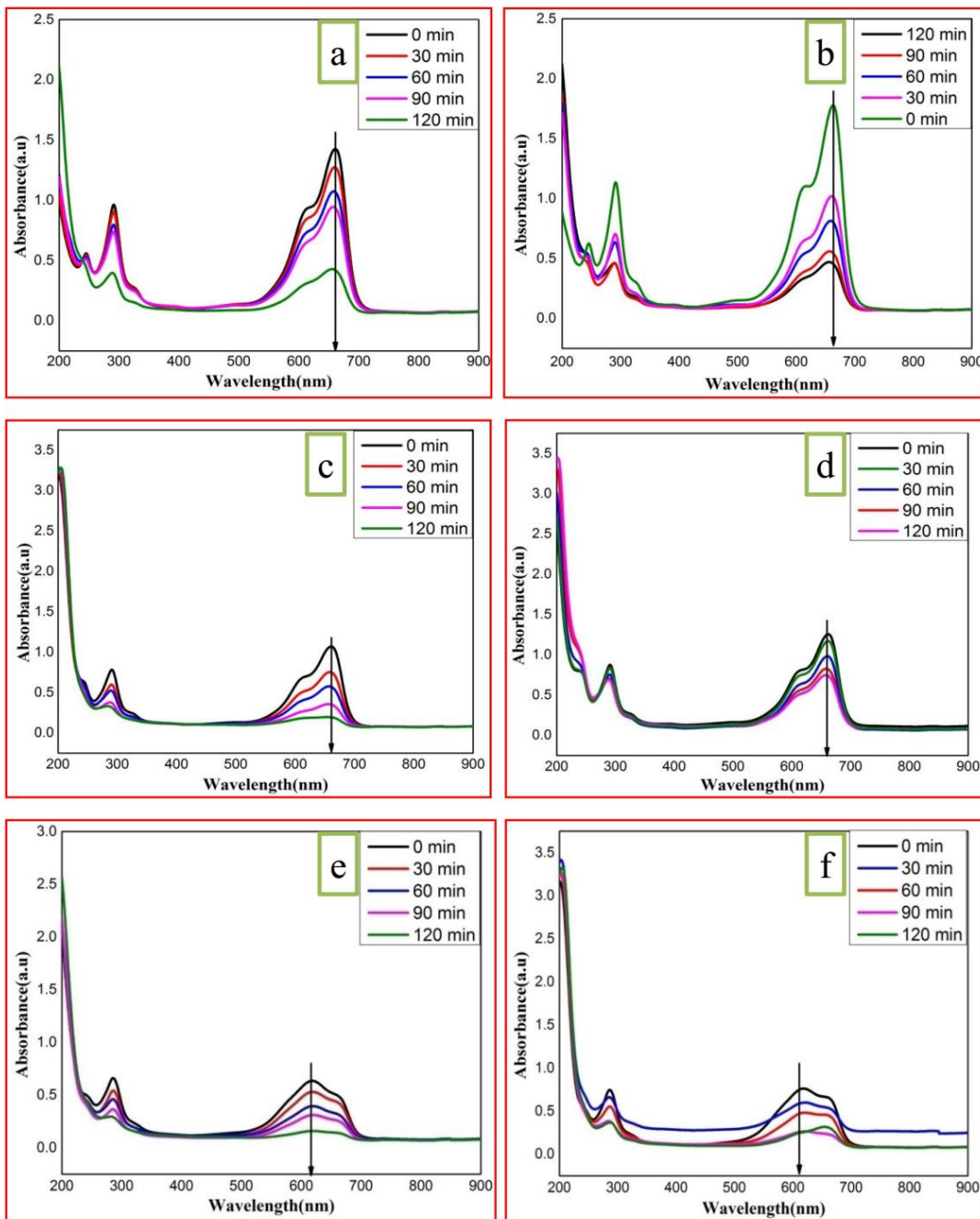


**Figure 9** (a-f) UV visible absorption spectra of (a) Pure CdO and (b-f) various concentration of *HRS* leaf extract CdO nanoparticles.

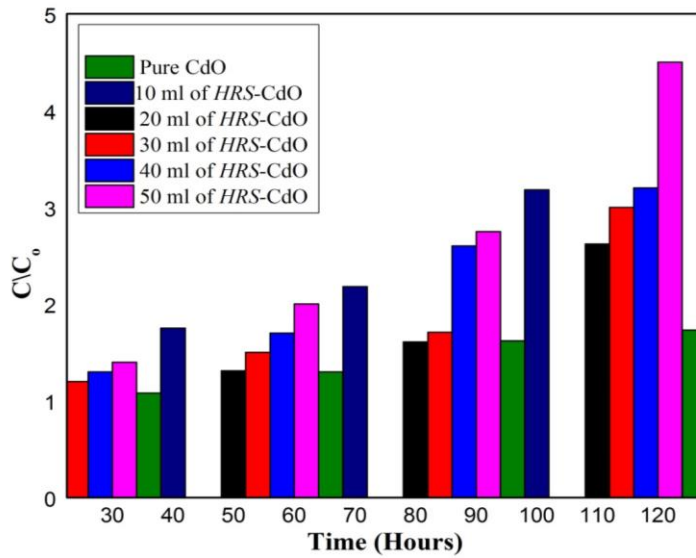


Figure 10 shows the photodegradation of Methylene blue.

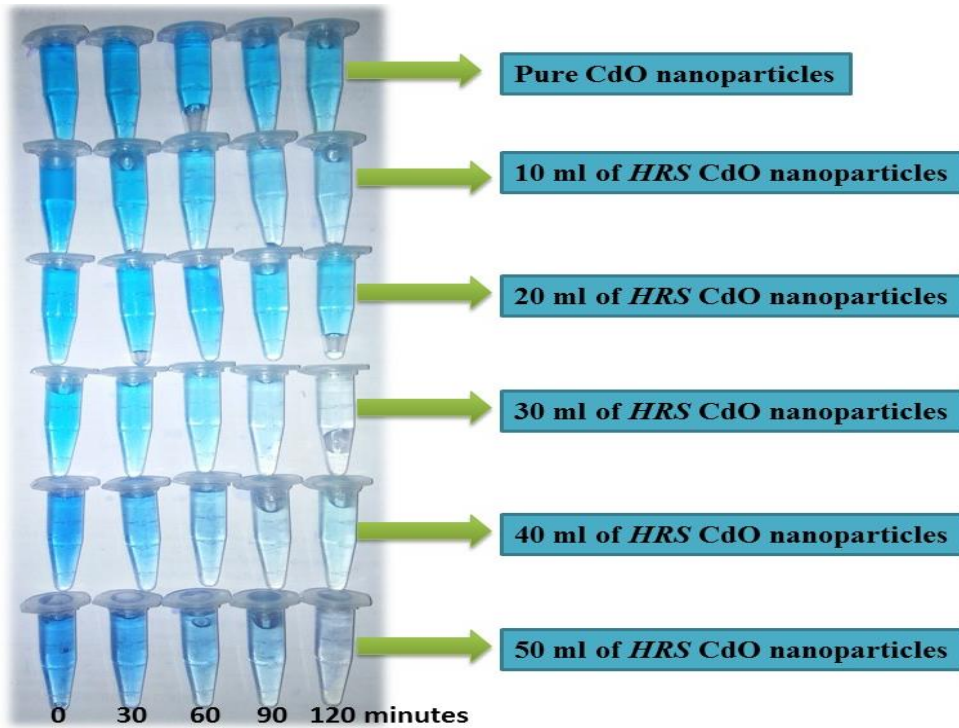
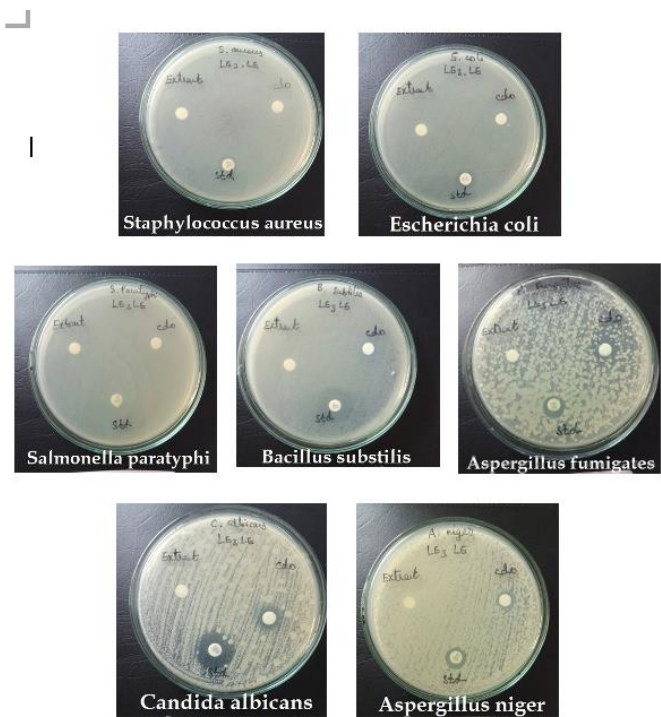
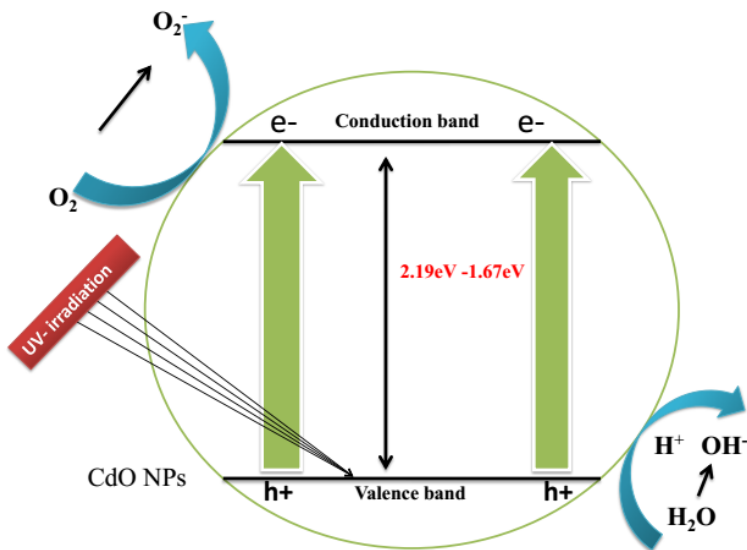


Figure 11 shows the photographic image photodegradation of Methylene blue.

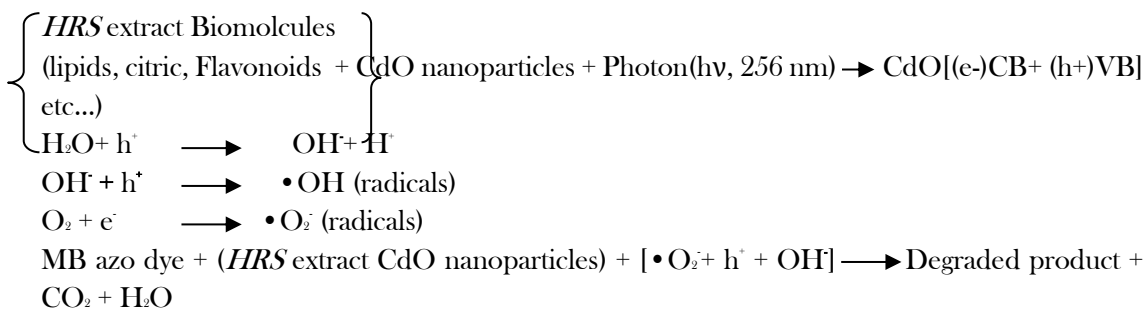


**Figure 12** Photograph showing Anti-bacterial and Anti-Fungal activities of using *HRS* leaf extract CdO nanoparticles against different pathogenic microorganisms



**Scheme 1** Photocatalytic reaction mechanisms of HRS leaf extract CdO nanoparticles

The degradation mechanism of MB dye with pure CdO nanoparticles and different concentration of *HRS* leaf extract CdO nanoparticles under UV light irradiation are shown in Fig.10&11 and scheme (1). When the mixed solution of MB dye and photocatalyst (pure CdO, 10-50 ml of *HRS* leaf CdO nanoparticles) is exposed under UV light with excited to the CB wavelength 365 nm; the  $e^-$  of VB is excited to the CB of CdO nanoparticles. The excited  $e^-$  will react with absorbed  $O_2$  molecules and form  $\bullet O_2^-$  radicals [47]. On another side, the  $h^+$  of VB of CdO nanoparticles are taken by OH derived from the aqueous solution and form  $\bullet OH$  radicals in the mixed solution [48]. These radicals ( $\bullet O_2^-$  and  $\bullet OH$ ), act as oxidizing agents. These radicals react with MB dye molecules and decompose it into  $CO_2$ ,  $H_2O$  and other small molecules. The recombination time of  $e^-$ ,  $h^+$  pairs is little slow for pure CdO nanoparticles than the *HRS* leaf extract based CdO nanoparticles. The fast recombination of  $e^-$ ,  $h^+$  pairs quickly responded for the degradation process [46, 49]. The combination of *HRS* leaf extract and CdO nanoparticles prolonged the process of  $e^-$ ,  $h^+$  pairs, resulting enhanced photo degradation of MB dye with *HRS* leaf extract CdO nanoparticles. In the *HRS* leaf extract CdO nanoparticles, the biomolecules act as acceptor and transporter of electrons due to nice interfacial contact between MB dye and CdO nanoparticles. As a result, the electrons of CB of CdO nanoparticles may easily transfer to the biomolecules of the *HRS* leaf extract and prolonged the recombination process of  $e^-$ ,  $h^+$  pairs. The complete degradation process of MB dye in presence of *HRS* leaf extract CdO nanoparticles as a photocatalyst may be explained with the help of following equation,



These outcomes confirmed that this *HRS* leaf extract based CdO nanoparticles and their biomolecules will also be effectively elevated to the progress of photocatalytic activity which may also be supported one in the other way to produce clean environment.

## Conclusion

The CdO nanoparticles were synthesized by adopting the bio-green method using Hibiscus rosa sinensis leaf extract. The effect of pure and various concentration of *HRS* leaf extract CdO nanoparticles was investigated. The effective role of natural extract concentration is identified from the formation of good crystalline and higher particle size. The bandgap energy is also decreased due to increase in particles size which confirms the impact of natural bio extract.

The morphological modification is another significant factor which is observed from this study. The tetrahedral clog shaped crystalline structure embedded with CdO spherical nanoparticles has come to existence only due to utilization of HRS leaf extract. The TEM image is confirmed the particle size of CdO nanoparticles is measured as  $\sim 45$  nm. This HRS leaf extract CdO nanoparticles showed significant bacterial effect against both gram positive and gram negative strains and effective fungal activities. The CdO nanoparticles also possessed good photocatalytic activity on degradation of MB dye under UV light irradiation. Further it confirms that use of 50 ml HRS leaf extract on the preparation of CdO nanoparticles exhibit the highest photocatalytic activity. Thus, green synthesis process based on HRS leaf extract for CdO nanoparticles preparation is cost effective, simple, easily preparation and eco- friendly method..

## References

- [1] D.Sathya Raj et.al, Impact of n-heptane as surfactant in the formation of CdO nanowires through microwave combustion, *Applied Surface Science*, 266 (2013) 268-271.
- [2] S.Sivakumar et.al, Synthesis, characterizations and anti-bacterial activities of pure and Ag doped CdO nanoparticles by chemical precipitation method, *Spectrochimica Acta Part A: Molecular and Biomolecular Spectroscopy*, 136, Part C (2015) 1751-1759.
- [3] Payam Margan et.al, Sono-co precipitation synthesis and physicochemical characterization of CdO-ZnO nanophotocatalyst for removal of acid orange 7 from wastewater, *Ultrasonics Sonochemistry*, 40, Part A (2018) 323-332.
- [4] Jeevitesh K et.al, Influence of sol concentration on CdO nanostructure with gas sensing application, *Applied Surface Science*, 409 (2017) 8-16.
- [5] K.Anandhan et.al, Synthesis, FTIR, UV-Vis and Photoluminescence characterizations of triethanolamine passivated CdO nanostructures, *Spectrochimica Acta Part A: Molecular and Biomolecular Spectroscopy*, 149 (2015) 476-480.
- [6] Kezhen Qi et.al, Review on the improvement of the photocatalytic and antibacterial activities of ZnO, *Journal of alloys and compounds*, 727 (2017) 792-820.
- [7] S. Ambika et.al, Plant- extract mediated synthesis of ZnO nanoparticles using *Pongamia pinnata* and their activity against pathogenic bacteria., *Advanced Powder Technology*, 26 (2015) 1294-1299.
- [8] K.Kombaiah et.al, Studies on the microwave assisted and conventional combustion synthesis of *Hibiscus rosa sinensis* Plant extract based ZnFe<sub>2</sub>O<sub>4</sub> nanoparticles and their optical and magnetic properties, *Ceramics international*, 42 (2016) 2741-2749.
- [9] Renata Dolant et.al, Biosynthesis and antibacterial activity of ZnO nanoparticles using *Trifolium Pratense* flower extract, *Saudi journal of biological sciences*, 23 (2016) 517-523.
- [10] K.Elumalai et.al, Facile, eco-friendly and template free photosynthesis of cauliflower like ZnO nanoparticles using leaf extract of *Tamarindus indica* (L.) and its biological evolution of antibacterial and antifungal activities, *Spectrochimica Acta Part A: Molecular and Biomolecular Spectroscopy*, 136 (2015) 1052-1057.

- [11] Li Fu et.al, *Plectrans amboinicus* leaf extract- assisted biosynthesis of ZnO nanoparticles and their photocatalytic activity, *Ceramics international*, 41(2015) 2492-2496.
- [12] Zhong- Yin Zhao et.al, *Tribulus terrestris* leaf extract assisted green synthesis and gas sensing properties of Ag- coated ZnO nanoparticles, *Materials Letters* 158 (2015) 274-277.
- [13] Saeed jafarirad et.al, Biofabrication of Zinc oxide nanoparticles using fruit extract of *Rosa canina* and their toxic potential against bacteria: A mechanistic approach, *Materials Science& Engineering C*, 59, (2016) 296-302.
- [14] Evi Maryanti et.al, Synthesis of ZnO nanoparticles by hydrothermal method in aqueous rinds extract of *Sapindus rarak* DC, *Materials Letters* 118 (2014) 96-98.
- [15] M.Ramesh et.al, Green synthesis of ZnO nanoparticles using *Solanum nigrum* leaf extract and their antibacterial activity, *Spectrochimica Acta Part A: Molecular and Biomolecular Spectroscopy*, 136, Part B (2015) 864-870.
- [16] Xiao Dan Sun et.al, capturing tobacco specific N-nitrosamines (TSNA) in industrial tobacco extract solution by ZnO modified activated carbon. *Microporous and Mesoporous Materials* 222 (2016) 160-168.
- [17] F.T.Thema et.al, Green synthesis of ZnO nanoparticles via *Agathosma betulina* natural extract, *Materials Letters* 161 (2015) pages 124-127.
- [18] B.H.Patel et.al, Biosynthesis of copper nanoparticles; its characterization and efficacy against human pathogenic bacterium, *Journal of Environmental Chemical Engineering* 4, Issue 2 (2016) 2163-2169.
- [19] A.Vishnu Kirthi, A.Abdul Rahuman, G.Rajakumar, S.Marimuthu, T.Santhoshkumar, C.Jayaseelan,G.Elango, A.Abduz Zahir, C.Kamaraj, A.Bagavan., Biosynthesis of titanium dioxide nanoparticles using bacterium *Bacillus subtilis*., *Materials Letters* 65(2011)2745-2747.
- [20] Bonnia N.N, Kamaruddin M.S, Nawawi M.H, S,Ratim, H.N Azlina, and Ali E.S., Green Biosynthesis of Silver nanoparticles Using ‘polygonum Hydropiper’ And Study Its Ctalytic Degradation of Methylene Blue, *Procedia Chemistry* 19(2016) 594-602.
- [21] Mostafa M.H.Khalil, Eman H. Ismail, Fatma EI-Magdoub., Biosynthesis of Au nanoparticles using olive leaf extract, *Arabian journal of chemistry*(2012) 5, 431-437.
- [22] Vipin Kumar et.al, Structural, optical and electrical characterization of nanocrystalline CdO films for device applications *Optik - International Journal for Light and Electron Optics*, 127, Issue 10 (2016) 4254-4257.
- [23] C.C.Vidyasager et.al, Solid state synthesis and effect if temperature on optical properties of Cu-ZnO, Cu-CdO and CuO nanoparticles, *Power Technology* 214(2011) 337-343.
- [24] Kun Peng et.al, preparation of CdO hollow microsphere via H<sub>2</sub>O<sub>2</sub> pre-oxidation, *Materials Letters* 118(2014) 180-183.
- [25] Tokker Ahamad et.al, Biosynthesis, structural characterization and antimicrobial activity of gold and silver nanoparticles, *Colloids and Surfaces B: Biointerfaces*107 (2013) 227-234.

- [26] Anil Kumar et.al, Review on *hibiscus rosa sinensis*, International journal of Research in Pharamaceutical and Biomedical sciences. ISSN: 229-3701.
- [27] Daizy Philip, Green synthesis of gold and silver nanoparticles using *Hibiscus rosa sinensis*, Physica E 42(2010) 1417-1424.
- [28] S. Ambika et.al, Green synthesis of ZnO nanoparticles using Vitex negundo L.extract: Spectroscopic investigation between ZnO nanoparticles and human serum albumin, Journal of Photochemistry and Photobiology B: biology 149 (2015) 143-148.
- [29] N. Thovhogi et.al, Physical properties of CdO nanoparticles synthesized by green chemistry via *Hibiscus Sabdariffa* flower extract, Journal of Alloys and Compounds 655(2016) 314-320.
- [30] ShakeelAhmed et.al, A review on biogenic synthesis of ZnO nanoparticles using plant extracts and microbes: A prospect towards green chemistry, Journal of Photochemistry and Photobiology B: Biology, 166 (2017) 272-284.
- [31] A facile method to synthesis of CdO nanoparticles from spent Ni-Cd batteries, Gholam Reza Khayati et.al, Materials Letters, 115 (2014) 272-274.
- [32] Eco-friendly synthesis of ZnO nanoparticles with different morphologies and their visible light photocatalytic performance for the degradation of Rhodamine B, Sana Akir et.al, Ceramics International, 42, Issue 8 (2016) 10259-10265.
- [33] *Caralluma fimbriata* extract induced green synthesis, structural, optical and photocatalytic properties of ZnO nanostructure modified with Gd Preeti Mishra et.al, Journal of Alloys and Compound, 685 (2016) 656-669.
- [34] K. Elumalai et.al, Bio-approach: Plant mediated synthesis of ZnO nanoparticles and their catalytic reduction of methylene blue and antimicrobial activity, Advanced Powder Technology., 26, Issue 6 (2015) 1639-1651.
- [35] D. Suresh et.al, Chironji mediated facile green synthesis of ZnO nanoparticles and their photoluminescence, photodegradative, antimicrobial and antioxidant activities, Materials Science in Semiconductor Processing, 40 (2015) 759-765.
- [36] R. Pandimurugan et.al, Novel seaweed capped ZnO nanoparticles for effective dye photodegradation and antibacterial activity, Advanced Powder Technology. 27, Issue 4, (2016)1062-1072
- [37] Thenmozhi Karnan et.al, Biosynthesis of ZnO nanoparticles using rambutan (*Nephelium lappaceumL.*) peel extract and their photocatalytic activity on methyl orange dye, Journal of Molecular Structure, 1125 (2016) 358-365
- [38] A comparative study of the synthesis of CdO nanoplatelets by an albumen-assisted isothermal evaporation method, T.Prakash et.al, Journal of Alloys and Compounds 624, (2015) 258-265.
- [39] Susan Azizi et.al, Effect of annealing temperature on antimicrobial and structural properties of Bio-synthesized Zinc Oxide Nanoparticles Using Flower Extract of *Anchusa Italic*, Photochemistry and photobiology, 161 (2016) 441-449.



- [40] D Philip, Biosynthesis of Au, Ag and Au-Ag nanoparticles using edible mushroom extract. Spectrochim. Acta A 73, (2009) 374–381.
- [41] D Raghunandan, S Basavaraja, B Mahesh, S Balaji, SY Manjunath, A Venkataraman, Biosynthesis of stable polyshaped gold nanoparticles from microwave-exposed aqueous extracellular anti-malignant guava (*Psidium guajava*) leaf extract. Nano Biotechnol. 5(1–4), (2009) 34–41.
- [42] Akbar Yasmin, Kumaraswamy Ramesh and Shanmugam Rajeshkumar, Yasminetal, Optimization and stabilization of gold nanoparticles by using herbal plant extract with microwave heating, Nano Convergence 1, 12 (2014).
- [43] Kristýna Večeřová et.al, Changes of primary and secondary metabolites in barley plants exposed to CdO nanoparticles, Environmental Pollution, 218 (2016) 207-218.
- [44] K. Elumalai et.al, Facile, eco-friendly and template free photosynthesis of cauliflower like ZnO nanoparticles using leaf extract of *Tamarindus indica* (L.) and its biological evolution of antibacterial and antifungal activities, Spectrochimica Acta Part A: Molecular and Biomolecular Spectroscopy. 136, Part B, (2015) 1052-1057.
- [45] Cao YW, Jin R, Mirkin CA. DNA modified core-shell Ag/Au nanoparticles. J Am Chem Soc 2001; 123:7961-2.
- [46] Gopi Somasundaram, jayaprakash rajan, Effectual Role of *Abelmoschus esculentus* (Okra) Extract on Morphology, Microbial and Photocatalytic Activities of CdO Tetrahedral Clogs, J.Inorg Organomet Polym 28 (2018) 152–167.
- [47] T.Linda et.al, Fabrication and characterization of chitosan templated CdO/NiO nano composite for dye degradation, Optik, 127, Issue 20 (2016) 8287-8293.
- [48] C. Maria Magdalane et.al, Photocatalytic degradation effect of malachite green and catalytic hydrogenation by UV-illuminated CeO<sub>2</sub>/CdO multilayered nanoplatelet arrays: Investigation of antifungal and antimicrobial activities, Journal of Photochemistry and Photobiology B: Biology, Volume 169, April 2017, 110-123.
- [49] P.Senthil Kumar et.al, CdO nanospheres: Facile synthesis and bandgap modification for the superior photocatalytic activity, Materials Letters, 151(2015) 45-48.

**Funding:** No funding was received for conducting this study.

**Conflict of interest:** The Authors have no conflicts of interest to declare that they are relevant to the content of this article.

**About The License:** © The Author(s) 2022. The text of this article is open access and licensed under a Creative Commons Attribution 4.0 International License